HIGH-STRESS FATIGUE EXPERIMENTS ON SINGLE CRYSTAL SILICON IN AN OXYGEN-FREE ENVIRONMENT

V.A. Hong[1], S. Yoneoka[1,2], M.W. Messana[1,3], A.B. Graham[1,4], J.C. Salvia[1,5], T.T. Branchflower[1], E.J. Ng[1], and T.W. Kenny[1]

[1]Stanford University, USA, [2]now at mCube Inc, USA, [3]now at Skybox Imaging, Inc, USA, [4]now at Robert Bosch LLC Research and Technology Center, USA, [5]now at SiTime Corporation, USA

ABSTRACT

In this paper we present the first fatigue study with stress loadings above 2 GPa applied to single-crystal silicon (SCS) resonators in an inert environment provided by the 'epi-seal' encapsulation process. In total, 6 devices representing a total of 16 experiments were actuated for $>10^{10}$ cycles with stress levels >3.2 GPa at 32°C. No fatigue-like behavior was observed up to 7.5 GPa, which is far beyond the threshold for fatigue reported by others. High-cycle fatigue in SCS is therefore likely to be a surface or environmentally-assisted phenomenon that can be minimized using better packaging techniques, such as 'epi-seal'.

INTRODUCTION

Background

MEMS-based sensors and actuators made from single-crystal silicon (SCS) are commonly subjected to high-cycle loadings. Understanding and preventing microscale fatigue of SCS therefore plays a large role in the MEMS design process to ensure the long-term stability and reliability of a device. To prevent SCS fatigue, devices are designed to operate below stress levels in which fatigue has been witnessed with the appropriate safety factor. Characterizing these fatigue-inducing stress levels is thus important to allow devices to extract more performance, and has subsequently been a topic of research for the past 20 years.

Since Connally and Brown's seminal work in 1992 [1], there have been many reports of SCS fatigue [2-13]. Several fatigue mechanisms have been proposed; the predominate ones being the reaction layer model from Muhlstein *et al.* [2] and the subcritical cracking model from Kahn *et al.* [3]. The reaction layer model asserts that a crack occurs in a native oxide layer and the oxide layer thickens due to SCS exposure to moisture or oxygen. Fatigue of SCS ensues due to repeated cracking and oxide-thickening until the crack has reached a critical length, leading to catastrophic failure of the device. Alternatively, the subcritical cracking model asserts that fatigue cracks occur in the silicon. It is proposed that compressive stresses promote crack extension in the silicon itself due to the increased stress intensity brought on by a wedging effect of native oxide or wear debris. These two fatigue mechanisms center around the effects of surface oxide, humidity and oxygen, and their exact roles remain controversial.

'Epi-seal' encapsulation

The 'epi-seal' encapsulation process developed at Stanford enables the packaging of an oxide-free MEMS device in an environment that is free of humidity, oxygen, and organics [14], thus eliminating the main factors that other researchers have attributed to long-term fatigue.

Previous experiments performed by Yoneoka *et al.* using devices fabricated in the 'epi-seal' process confirmed the absence of SCS fatigue using this encapsulation technique, however, the geometry of these devices limited stress levels to <2 GPa [12]. Devices were unable to be actuated beyond the 3.2 GPa in which other researchers have always witnessed fatigue, as seen in Fig. 6.

In this work wedge-shaped resonators, a design commonly used in MEMS fatigue testing, were fabricated using the 'epi-seal' encapsulation process. The geometry of the comb fingers was modified to accommodate larger stress levels than from Yoneoka *et al.* Devices were subjected to fully-reversed stresses and resonant frequency change was monitored using an oscillator circuit with automatic gain control (AGC).

DESIGN

Fatigue test resonators with resonant frequencies between 60 kHz and 70 kHz were designed and fabricated on a 20 µm thick device layer. The test structure consists of a wedge-shaped proof mass connected to the anchor with a cantilever. A V-shaped notch, with depth, *d*, of 7.5 µm and radius, *r*, of 0.5 µm, is placed on the cantilever to concentrate stress. The cantilever, aligned in the <110> direction, has a width, *w*, of 15 µm and length, *l*, of 30 µm. The overall length of the structure, including the proof mass, is 300 µm. Because of design rules that limit the structure's release area, the proof mass was designed in a Y-shape to accommodate a support for the cap layer. The proof mass, which has comb fingers, is electrostatically actuated on one side by a stationary drive electrode. On the other side a stationary electrode senses the displacement by measuring the change in capacitance between the proof mass and electrode when the resonator is driven.

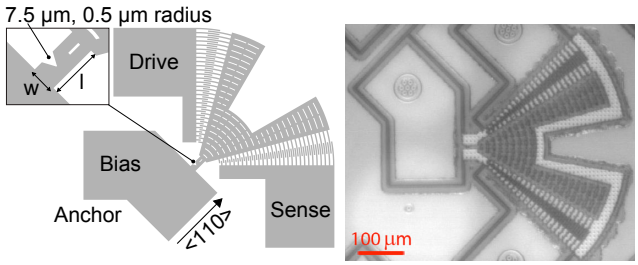

Figure 1: (a) Design of wedge-shaped resonator used as the fatigue structure. (b) Infrared image of a fabricated fatigue structure.

FABRICATION

The fatigue test resonators were fabricated using a process developed by Messana *et al.* [15] that combined traditional 'epi-seal' encapsulation with wafer bonding. Devices were defined with a deep reactive-ion etch and were sealed using a combination of fusion wafer bonding and epitaxially grown silicon, resulting in a SCS cap layer, as shown in Fig. 2. The wafers are sealed at 1130 °C in a hydrogen ambient (20 Torr), resulting in an oxide-free device and cavity free of oxygen and humidity. The wafers were subsequently annealed for more than 100 hours to diffuse out residual hydrogen, thereby reducing cavity pressure and increasing the quality factor of the resonators.

Furthermore, resonators fabricated using this encapsulation technology have demonstrated no discernable inherent aging or drift at the ppm-level under low stresses (<150 MPa) over 416 days of continuous operation [16], providing a robust platform for investigating fatigue-related effects at higher stress levels.

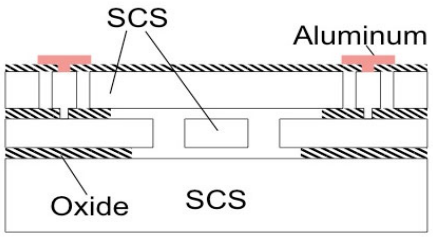

Figure 2: Cross-section schematic of 'epi-seal' encapsulation with SCS device and cap. The device layer thickness is approximately 20 μm.

EXPERIMENTAL SETUP

Oscillator Setup

The resonators are driven with a fully-reversed (R = -1), constant amplitude sinusoidal signal in a close-loop oscillator employing AGC, as shown in Fig. 3. V_{SET} controls the amplitude of the drive signal, V_{AC}, and a DC bias voltage, V_{bias}, enables electrostatic actuation; moreover, adjusting this voltage allows for control of the applied stress level. A counter and multimeter are placed after the transimpedance-amplifier (TIA) to measure frequency and RMS voltage of the output signal from the resonator. Any fatigue-like behavior is detected using the measured frequency, as changes in stiffness or mass would immediately be reflected in the resonant frequency; fatigue would be marked by a downward drift in frequency

During experimentation, four resonator-oscillator circuits were placed in a temperature chamber kept at 32 ± 0.1°C. A multiplexer enables switching between each resonator-oscillator setup, which allows for monitoring of devices with a single counter and multimeter.

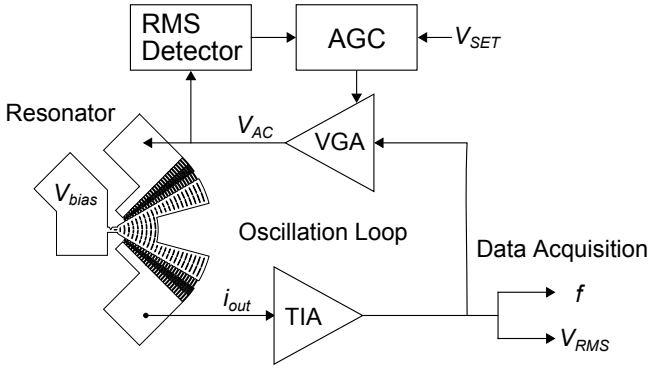

Figure 3: Block diagram of oscillator loop used to drive the resonator. The AGC loop allows for constant AC voltage input by using a variable gain amplifier (VGA).

Stress Calculation

Though 'epi-seal' provides a robust platform for device packaging, the encapsulation does not allow for direct measurement of stress, therefore stress at the notch must be calculated based on the resonator's electrical output signal, namely the frequency and amplitude.

The measured current arises due to time-varying capacitance at the sense electrode and is given by the following relation,

$$i_{out} = \frac{\partial Q}{\partial t} = V_{bias}\frac{\partial C}{\partial \theta}\frac{\partial \theta}{\partial t} = V_{bias}\frac{\partial C}{\partial \theta}\theta_{amp} j\omega e^{j\omega t}, \quad (1)$$

where Q is charge, t is time, θ is angle, θ_{amp} is maximum angular displacement, V_{bias} is bias voltage, C is the total capacitance of the comb fingers, and ω is angular frequency. The capacitance is calculated by approximating the comb fingers as cylindrical plates and summing over all combs, as shown in the following:

$$C = \sum_k \frac{\varepsilon h \theta}{\ln(r_{o,k}/r_{i,k})}, \quad (2)$$

where ε is permittivity, h is device thickness, $r_{o,k}$ is the outer radius for specific comb finger k, and $r_{i,k}$ is the inner radius for specific comb finger k.

From Eq. (1), the current amplitude, i_{amp}, is calculated from the measured RMS voltage, V_{RMS}, and the current-to-voltage transfer function, $G(j\omega)$ of the TIA, shown as

$$i_{amp} = \frac{\sqrt{2}V_{RMS}}{G(j\omega)} = V_b \frac{\partial C}{\partial \theta}\theta_{amp}\omega. \quad (3)$$

θ_{amp} is then determined and stress at the notch is subsequently calculated based on a FEA-modeled transfer function of 2.82 GPa/°.

RESULTS AND DISCUSSION

During experimentation, the fatigue structures were subjected to cyclic stress amplitudes of up to 7.5 GPa. Fig. 4 is a representative data set that shows frequency change (Δf), stress amplitude, bias voltage, and temperature monitored over a period of greater than 10 days. Δf is a normalized frequency change, defined as ppm = $10^6 \times (f - f_0)/f_0$, where f_0 is the initial frequency.

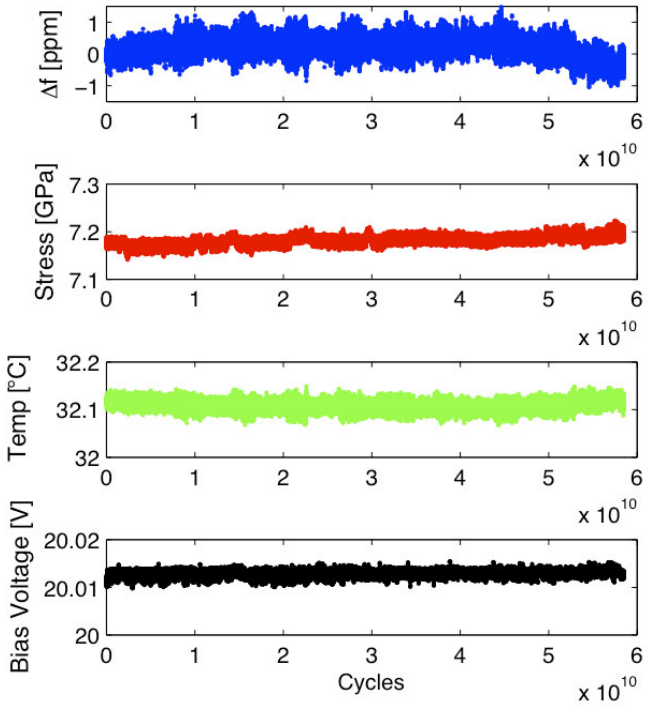

Figure 4: A representative data set, including plot of frequency change in ppm, stress amplitude at notch, temperature, and bias voltage over 6×10^{10} actuation cycles (>10 days).

No fatigue related behavior was observed in any of our experiments. Fluctuations in frequency at the ppm-level can be attributed to temperature or bias voltage noise. Furthermore, a linear fit of Δf vs. cycles (normalized to 10^{10} cycles) was performed to examine whether device frequencies drifted due to long-term fatigue damage. Fig. 5 shows that although devices exhibited negative frequency drifts, these drifts were smaller than the noise level (±1.3 ppm) at 32°C. In addition, there was no correlation between drift and stress amplitude, which would be expected in the case of fatigue. These results confirm that SCS is not susceptible to long-term fatigue damage.

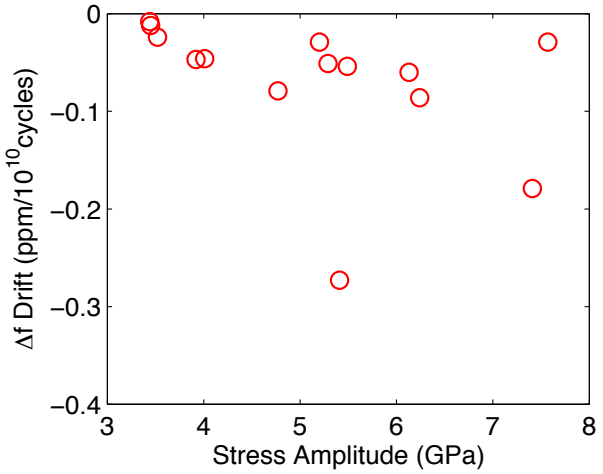

Figure 5: Calculation of frequency drift normalized over 10^{10} cycles from various fatigue test experiments with different stress amplitude loadings.

Cross-Comparison Summary

Fig. 6 shows a cross-comparison between this work and data presented from literature. The 'target' region in the top-right corner marks an area in which other researchers always witnessed fatigue failure, both in terms of stress (>3.2 GPa) and number of cycles (>10^{10}). These other works witnessed fatigue under varying conditions, but none of these experiments are as controlled as the inert environment and pristine device surface provided by 'epi-seal' encapsulation.

When compared against other works that reported fatigue [9-13] at temperatures between 22-30°C, our devices were subjected to higher stress levels and cycles without onset of fatigue failure. In total, 6 different devices from this work were tested in the 'target' region, making up a total of 16 experiments in which no fatigue failure occurred. Applying higher bias voltages to achieve stress levels above 7.5 GPa resulted in either immediate mechanical fracture or electrical pull-in of the comb fingers; since these results are not due to fatigue failure, they are not presented in Fig. 6.

CONCLUSION

This work presents a packaging technique that allows for single-crystal silicon devices to be actuated at stress amplitudes up to 7.5 GPa without the onset of high-cycle fatigue. We conclude that fatigue failure at room temperature (<32°C) witnessed from other works is either a surface or environmentally assisted phenomenon that can be eliminated with the 'epi-seal' encapsulation process. This important result allows for MEMS designers to extract more performance from current designs and allows for greater flexibility in design guidelines for MEMS devices experiencing high cyclic loading.

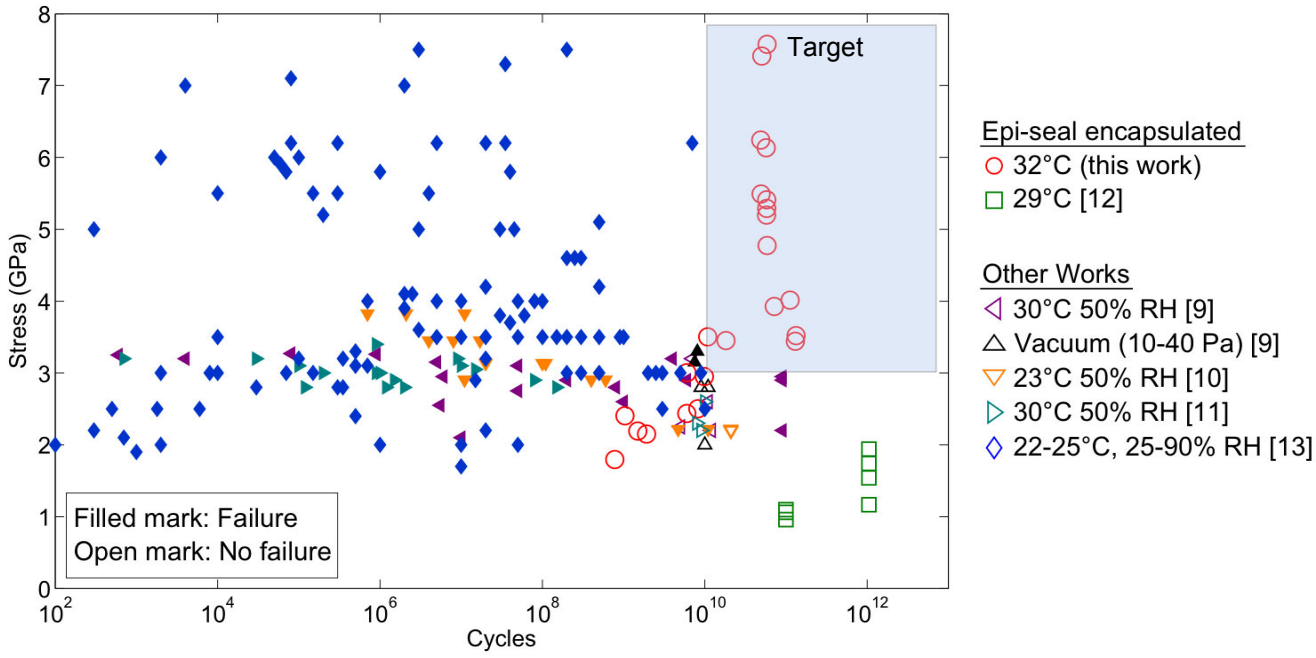

Figure 6: Stress-life (S-N) plot of data from various studies. All tests from this paper are run-out points (open mark), in which no sign of failure was observed. The "target" region represents stress levels in which other research groups always witnessed failure. We tested 6 different devices constituting 16 experiments in that region with no failure, providing an important design guideline for future MEMS designers.

ACKNOWLEDGEMENTS

This work was supported by the Defense Advanced Research Projects Agency (DARPA) thorough the N/MEMS S&T Fundamentals Program, managed by Dr. Tayo Akinwande. Student support was provided by a National Science Foundation Graduate Research Fellowship (VAH). The authors would like to thank Prof. R.T. Howe and H.K Lee for advice and guidance. Travel support has been generously provided by the Transducer Research Foundation.

REFERENCES

[1] J.A. Connally and S.B. Brown, "Slow crack growth in single-crystal silicon," Science, vol. 256, pp. 1537-1539, 1992.

[2] C.L. Muhlstein, E.A. Stach, and R.O. Ritchie, "A reaction-layer mechanism for the delayed failure of micron-scale polycrystalline silicon structural films subjected to high-cycle fatigue loading," Acta Mater., vol. 50, pp. 3579-3595, 2002.

[3] H. Kahn, R. Ballarini, J.J. Bellante, and A.H. Heuer, "Fatigue failure in polysilicon not due to simple stress corrosion cracking," Science, vol. 298, pp. 1215-1218, 2002.

[4] H. Kahn, R. Ballarini, and A.H. Heuer, "Dynamic fatigue in silicon," Curr. Opin. Solid in State Mater. Sci., vol. 9, pp. 71-76, 2004.

[5] C.L. Muhlstein, S.B. Brown, and R.O. Ritchie, "High-cycle fatigue of single-crystal silicon thin films," J. Microelectromech. Syst., vol. 10, pp. 593-600, 2001.

[6] T. Ando, M. Shikida, and K. Sato, "Tensile-mode fatigue of silicon films as structural materials for MEMS," Sens. Actuators: A, vol. 93, pp. 70-75, 2001.

[7] A.M. Fitzgerald, R.S. Iyer, R.H. Dauskardt, and T.W. Kenny, "Subcritical crack growth in single-crystal silicon using micromachined specimens," J. Matter. Res., vol. 17, pp. 683-692, 2002.

[8] T. Namazu and Y. Isono, "High-cycle fatigue damage evaluation for micro-nanoscale single crystal silicon under bending and tensile stressing," MEMS '04, Maastricht, Netherlands, Jan. 25-29, 2004, pp. 149-152.

[9] O.N. Pierron and C.L. Muslstein, "The critical role of environment in fatigue damage accumulation in deep-reactive ion-etched single-crystal silicon structural films," J. Microelectromech. Syst., vol. 15, pp. 111-119, 2006.

[10] T. Ikehara and T. Tsuchiya, "High-cycle fatigue of micromachined single-crystal silicon measured using high-resolution patterned specimens," J. Micromech. Microeng., vol. 18, pp. 1-7, 2008.

[11] P.-O. Theillet and O.N. Pierron, "Fatigue rates of monocrystalline silicon thin film in harsh environments: Influence of stress amplitude, relative humidity, and temperature," Appl. Phys. Lett., vol. 94, 181915, 2009.

[12] S. Yoneoka, Y.Q. Qu, S. Wang, M.W. Messana, A.B. Graham, B. Kim, R. Melamund, G. Bahl, and T.W. Kenny, "High-cyclic fatigue experiments of single crystal silicon in an oxygen-free environment," MEMS '10, Wanchai, Hong Kong, Jan. 24-28, 2010, pp. 224-227.

[13] S. Kamiya, T. Tsuchiya, T. Ikehara, K. Sato, T. Ando, T. Namazu, and K. Takashima, "Cross comparison of fatigue lifetime testing on silicon thin film specimens," MEMS '11, Cancun, Mexico, Jan. 23-27, 2011, pp. 404-407.

[14] R.N. Candler, W.T. Park, H. Li, G. Yama, A. Partridge, M. Lutz, and T.W. Kenny, "Single wafer encapsulation of MEMS devices," IEEE Trans. Adv. Packag., vol. 26, pp. 227-232, 2003.

[15] M.W. Messana, A.B. Graham, S. Yoneoka, R.T. Howe, and T.W. Kenny, "Packaging of large lateral deflection MEMS using a combination of fusion bonding and epitaxial reactor sealing," Proc. Hilton Head Workshop, June 6-10, 2010, pp. 70-73.

[16] B. Kim, R.N. Candler, M. Hopcroft, M. Agarwal, W.-T. Park, and T.W. Kenny, "Frequency stability of wafer-scale film encapsulated silicon based MEMS resonators," Sens. Actuators: A, vol. 136, pp. 125-131, 2007.

[17] R. N. Candler, W.-T. Park, M. Hopcroft, B. Kim, and T. W. Kenny, "Hydrogen diffusion and pressure control of encapsulated MEMS resonators," Transducers '05, Seoul, Korea, June 5-9, 2005, pp. 920-923.

CONTACT

*V.A. Hong, tel: +1-619-885-7081; vuhong@stanford.edu